Uncovering the Interleukin-12 Pharmacokinetic Desensitization Mechanism and Its Consequences with Mathematical Modeling

Jonathon DeBonis[a], Omid Veiseh[a], and Oleg A. Igoshin[a,b]

[a]Department of Bioengineering, Rice University, Houston, Texas, USA.

[b]Center for Theoretical Biological Physics, Department of Chemistry, Department of Biosciences, Rice University, Houston, Texas, USA

Corresponding Author: Oleg Igoshin, igoshin@rice.edu, Department of Bioengineering, Rice University, Houston, Texas, USA.

Acknowledgments

This work was partly supported by the Welch Foundation (grant C-1995 to O.A.I.), and by the Advanced Research Projects Agency for Health (ARPA-H) under Award Number AY1AX000003. The content is solely the responsibility of the authors and does not necessarily represent the official views of the Welch Foundation or ARPA-H.

Conflicts of Interest

O.V. holds equity and O.A.I has a consultant position in Avenge Bio. The authors declare that they have no other competing interests.

Abstract

The cytokine interleukin-12 (IL-12) is a potential immunotherapy because of its ability to induce a Th1 immune response. However, success in the clinic has been limited due to a phenomenon called IL-12 desensitization – the trend where repeated exposure to IL-12 leads to reduced IL-12 concentrations (pharmacokinetics) and biological effects (pharmacodynamics). Here, we investigated IL-12 pharmacokinetic desensitization via a modeling approach to (i) validate proposed mechanisms in literature and (ii) develop a mathematical model capable of predicting IL-12 pharmacokinetic desensitization. Two potential causes of IL-12 pharmacokinetic desensitization were identified: increased clearance or reduced bioavailability of IL-12 following repeated doses. Increased IL-12 clearance was previously proposed to occur due to the upregulation of IL-12 receptor on T-cells that causes increased receptor-mediated clearance in the serum. However, our model with this mechanism, the accelerated-clearance model, failed to capture trends in clinical trial data. Alternatively, our novel reduced-bioavailability model assumed that upregulation of IL-12 receptor on T-cells in the lymphatic system leads to IL-12 sequestration, inhibiting the transport to the blood. This model accurately fits IL-12 pharmacokinetic data from three clinical trials, supporting its biological relevance. Using this model, we analyzed the model parameter space to illustrate that IL-12 desensitization occurs over a robust range of parameter values and to identify the conditions required for desensitization. We next simulated local, continuous IL-12 delivery and identified several methods to mitigate systemic IL-12 exposure. Ultimately, our results provide quantitative validation of our proposed mechanism and allow for accurate prediction of IL-12 PK over repeated doses.

24 **Introduction**

25 Inteleukin-12 (IL-12) is a 70 kDa heterodimeric cytokine consisting of a 35 kDa α subunit and a
26 40 kDa β subunit[1]. IL-12's immunological activity is characterized by causing differentiation of
27 CD4+ helper T-cells (Th-cells) into the Th1 phenotype, leading to the production of pro-
28 inflammatory cytokines and immune system activation[2]. The primary cytokine induced by IL-12
29 activity is IFNγ, but TNFα, GM-CSF, IL-2, and IL-8 are also known to be produced in response to
30 IL-12 stimulus[1,3]. Immune activation is achieved through the binding of IL-12 to its receptor,
31 which ultimately leads to the activation of STAT4[1,3,4]. IL-12's ability to trigger robust immune
32 system activation motivates its investigation as a potential cancer immunotherapy.

33 The first clinical trial investigating IL-12 was initiated in 1997 for the treatment of cancer patients
34 with advanced malignancies[1,5]. Here, patients were first treated with an i.v. test dose of IL-12 two
35 weeks before receiving five times weekly i.v. doses of IL-12 every 28 days[5]. A phase two trial was
36 initiated shortly after following the same dose regimen without the test dose. In stark contrast to
37 the phase one trial, this trial was quickly terminated after severe toxicities, including treatment-
38 related patient deaths[6]. It was apparent that prior exposure to IL-12 desensitizes patients to IL-
39 12's immunological activity, evident through the ~5-fold increase in measured serum IFNγ in
40 patients treated with the same dose in the PII trial.

41 IL-12 desensitization has been observed in a large number of additional clinical trials, with results
42 illustrating that both IL-12 pharmacokinetics (PK) and pharmacodynamics (PD) are desensitized[7–
43 16]. PD desensitization is characterized by reduced IFNγ levels following repeated doses[5,6,12,15],
44 whereas PK desensitization causes reduced IL-12 concentrations.[13,14,17]. Furthermore, PK and PD
45 desensitization appear to be caused by separate mechanisms due to a difference in the timescale in
46 which these phenomena occur. In a study of repeated subcutaneous IL-12 doses in mice, measured

47 serum IL-12 concentrations decreased with every dose administered, whereas measured serum
48 IFNγ concentrations decreased after three doses were administered[17]. Despite increasing tolerance
49 to IL-12 administration, studies have shown that response to IL-12 treatment is also hindered by
50 desensitization[10,12,18]. Ultimately, due to its implications in both tolerability and response to IL-12
51 treatment, understanding the mechanism causing PK and PD desensitization is essential for the
52 optimization of IL-12 therapies.

53 Several mechanisms have been proposed in the literature to explain IL-12 PK and PD
54 desensitization; however, none have been validated quantitatively. Importantly, results from
55 clinical trials illustrate that anti-drug antibodies (ADAs) are rarely formed against IL-12[5,9,13,17],
56 suggesting a different mechanism for desensitization. In terms of PK desensitization, the primary
57 molecular mechanisms discussed revolve around the upregulation of IL-12 receptors on T-cells
58 following IL-12 stimulation[13,19]. Increased expression of IL-12 receptor leads to higher levels of
59 receptor-mediated clearance, which can lead to faster serum clearance or higher levels of IL-12
60 sequestration during transport into the blood. Overall, this would lead to reduced serum IL-12
61 concentrations due to increased clearance or lower bioavailability, and these effects are apparent
62 almost immediately after repeated doses. Conversely, desensitization of IL-12's immunological
63 effects is delayed and tends to occur after several doses have been administered[13]. Discussed
64 mechanisms for this effect include downregulation of STAT4 after sustained IL-12 signaling[20] and
65 adaptive T-cell exhaustion due to IL-12 stimulation[8,16].

66 Here, focusing on PK desensitization, we investigated proposed mechanisms for IL-12 PK
67 desensitization in literature via a modeling approach. More specifically, we developed
68 mathematical models containing two different mechanisms of interest for IL-12 PK desensitization
69 and challenged these models to fit clinical trial data. Furthermore, after identifying the mechanism

70 that is consistent with the data, we determine the parameter regime under which significant
71 desensitization can occur and use the model with our proposed mechanism to identify potential
72 strategies for mitigating systemic toxicity to IL-12 treatment.

73 **Methods**

74 *Clinical Trial Data Collection*

75 Three clinical trials with IL-12 PK measurements over multiple subcutaneous doses of IL-12 were
76 identified. The first trial, presented by Motzer and colleagues, reports IL-12 PK in patients with
77 advanced renal cell carcinoma over three repeated doses on days 1, 8, and 15 of a 28-day cycle[13].
78 IL-12 was administered according to two dosing regimens: the fixed cycle with three equivalent
79 doses and the escalating cycle with doses incrementally increasing to a target amount on day 15.
80 IL-12 measurements in the blood were reported following the first dose in the fixed cycle or the
81 third dose in the escalating cycle. The second trial, presented by Rakhit and colleagues, contains
82 IL-12 PK following the same dosing schedule as the fixed cycle in the first trial but instead reports
83 IL-12 blood measurements after the first dose in cycle one and the third dose in cycle two[17]. The
84 third suitable trial, by Portielje and colleagues, presents PK measurements (C_{max}, AUC, t_{max}, $t_{1/2}$)
85 following the first and seventh doses in a cycle consisting of three s.c. doses of IL-12 each week
86 following a single priming dose one week before beginning the cycle[14,15]. In trials with time-
87 course data, the numerical values were extracted from figures using GraphGrabber2.0.2
88 (Quintessa).

89 *Mathematical Models of IL-12 PK and Numerical Simulation*

90 Two models containing separate molecular mechanisms for IL-12 PK desensitization were
91 developed. The first one, the accelerated-clearance model, is based on the mechanism in which IL-

12 binding to its receptor in circulation causes STAT4 activation and receptor upregulation. This model consists of the ordinary differential equations and algebraic relationships in equations 1-9.

$$\frac{dIL12_S}{dt} = -J_{BS}\, IL12_S - k_{DG}\, IL12_S \tag{1}$$

$$\frac{dIL12_B}{dt} = \frac{J_{BS}\, V_S}{V_B}\, IL12_S - k_{on}\, IL12_B\, R - k_{CB}\, IL12_B \tag{2}$$

$$\frac{dR}{dt} = \frac{N_{cells}}{V_L}\, k_R + \frac{N_{cells}}{V_L}\, \alpha\, pSTAT - k_{on}\, IL12_B\, R - k_{CR}\, R \tag{3}$$

$$\frac{dC}{dt} = k_{on}\, IL12_B\, R - k_{int}\, C \tag{4}$$

$$\tilde{C} = \frac{6.023e11\, V_L}{N_{cells}}\, C \tag{5}$$

$$pSTAT = \frac{\tilde{C}}{\tilde{C} + IC_{pSTAT}} \tag{6}$$

$$k_R = k_{CR}\, R_0 \tag{7}$$

$$k_{DG} = \frac{(1-F)}{F}\, J_{BS} \tag{8}$$

$$IL12_{S,0} = \frac{D}{V_S} \tag{9}$$

The second model used in this investigation is the reduced-bioavailability model. Here, a lymphatic system compartment is included where receptor binding and upregulation occur. This model consists of the ordinary differential equations and algebraic relationships in equations 10-19.

$$\frac{dIL12_S}{dt} = -J_{LS} IL12_S - J_{BS} IL12_S - k_{DG} IL12_S \tag{10}$$

$$\frac{dIL12_L}{dt} = \frac{J_{LS}\,V_S}{V_L}\,IL12_S - k_{on}\,IL12_L\,R - J_{BL}\,IL12_L \tag{11}$$

$$\frac{dR}{dt} = \frac{N_{cells}}{V_L}\,k_R + \frac{N_{cells}}{V_L}\,\alpha\,pSTAT - k_{on}\,IL12_L\,R - k_{CR}\,R \tag{12}$$

$$\frac{dC}{dt} = k_{on}\,IL12_L\,R - k_{int}\,C \tag{13}$$

$$\frac{dIL12_B}{dt} = \frac{J_{BL}\,V_L}{V_B}\,IL12_L - k_{CB}\,IL12_B \tag{14}$$

$$\tilde{C} = \frac{6.023e11\,V_L}{N_{cells}}\,C \tag{15}$$

$$pSTAT = \frac{\tilde{C}}{\tilde{C} + IC_{pSTAT}} \tag{16}$$

$$k_R = k_{CR}\,R_0 \tag{17}$$

$$k_{DG} = \frac{(1-F)}{F}\,J_{LS} \tag{18}$$

$$IL12_{S,0} = \frac{D}{V_S} \tag{19}$$

Derivations and justifications for the terms in both models are located in the supplementary text. For predictions regarding local, intraperitoneal delivery of IL-12, we modified the reduced-bioavailability model to represent constant IL-12 production in the peritoneal cavity. The equations in this model are modified to include a 0th-order production rate of IL-12 in the peritoneal cavity and are located in the supplemental text.

Models were simulated in MATLAB (R2020b) using the ODE solver ode15s. All option arguments are set to default except for the non-negative argument set to one and the absolute tolerance set to 1e-12.

Data Fitting and Parameter Estimation Procedures

We utilized two methods to fit our model to clinical trial data. Global optimization was implemented using MATLAB's particleswarm algorithm, and ensemble local optimization was implemented by randomly sampling parameter sets within optimization boundaries and locally optimizing using MATLAB's patternsearch algorithm[21].

The error functions used for optimization depend on the type of data and the number of compartments for which data was available. For time course data presented for a single compartment, we used a modified version of the sum of standard squared error to account for the assay's limit of detection:

$$SSE = \sum_i \begin{cases} (P_i - E_i)^2; P_i > D, E_i > D \\ (P_i - D)^2; P_i > D, E_i \leq D \\ 0; P_i \leq D, E_i \leq D \end{cases} \tag{20}$$

where E_i is the value of experimental datapoint i, P_i is the model predicted value of that datapoint, and D is the lowest limit of detection for the quantification assay. For time course data where data is presented for more than one compartment, i.e., blood and intraperitoneal IL-12 measurements, the error function was further modified to normalize to the magnitude of the experimental measurement according to equation 21.

$$NSE = \sum_i \begin{cases} \frac{(P_i - E_i)^2}{E_i^2}; P_i > D, E_i > D \\ \frac{(P_i - D)^2}{D^2}; P_i > D, E_i \leq D \\ 0; P_i \leq D, E_i \leq D \end{cases} \tag{21}$$

The error function used for optimizing to PK metric data is given by the following:

$$SSE = \sum_i \frac{(P_i - E_i)^2}{E_i^2 + \sigma_i^2} \tag{22}$$

138 Here, E_i is the value of the PK metric measured in the clinical trial, σ_i is the reported standard
139 deviation of the PK metric, and P_i is the model predicted value.

140 **Results**

141 *Two alternative models of desensitization describing literature-proposed mechanisms were*
142 *developed.*

143 We first identified proposed mechanisms for IL-12 PK desensitization in literature as a basis for
144 developing our mathematical models. Analysis of preclinical and clinical trials of IL-12 provided
145 evidence for two distinct causes of IL-12 PK desensitization: increased clearance or decreased
146 bioavailability following repeated doses[9,13,14,17]. While both were proposed in the literature,
147 neither cause has been validated quantitatively. Thus, we aimed to formulate molecular
148 mechanisms for the identified causes of IL-12 desensitization in literature and validate whether
149 these mechanisms can account for trends in clinical trial data.

150 Two models were constructed containing molecular mechanisms for increased clearance or
151 reduced bioavailabilty after repeated IL-12 doses, respectively. Both models contain equations
152 representing IL-12 dosing, transport, and degradation in the subcutaneous space. Furthermore, IL-
153 12 binding to IL-12 receptors on T-cells also occurs in both models. Formation of IL-12:IL-12
154 receptor complex activates STAT4 based on a quasi-steady state assumption, and STAT4 activation
155 upregulates the production of IL-12 receptor[14,17,19].

156 The main difference between the two models is the compartment where receptor binding and
157 upregulation occur. Our first model was designed such that upregulation of the IL-12 receptor on
158 T-cells leads to accelerated clearance of IL-12 from the serum. Accordingly, IL-12 binds its
159 receptor in the blood compartment such that clearance occurs from receptor binding and standard

first-order clearance/degradation. As no significant interactions occur in the lymphatic system

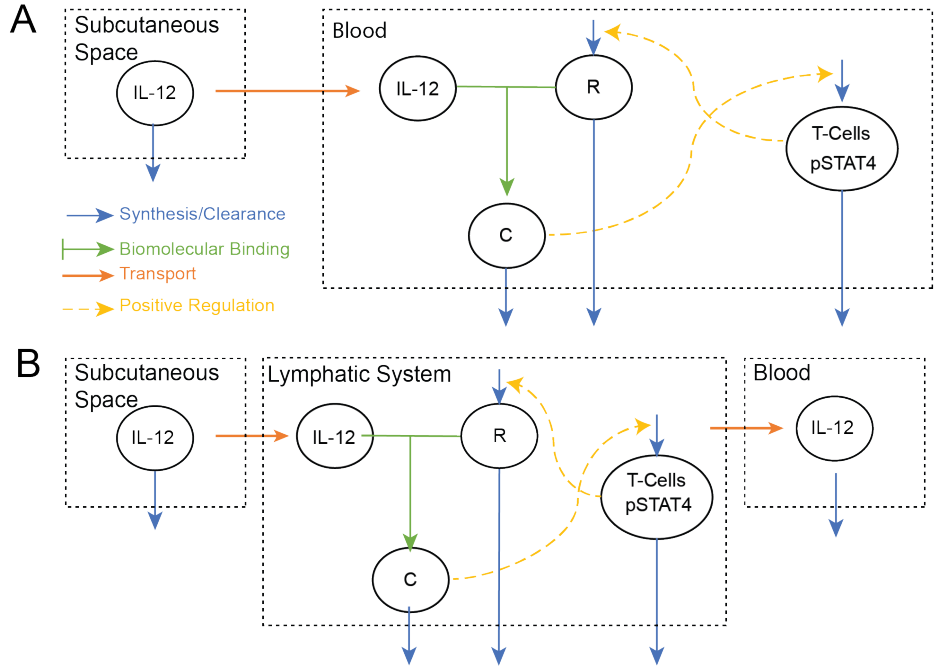

Figure 1: Schematics detailed two models developed in this investigation. A) Schematic of accelerated-clearance model. B) Schematic of reduced-bioavailability model.

based on this mechanism, the lymphatic system compartment is omitted from this model. Conversely, our second model was designed such that receptor upregulation leads to reduced bioavailability. In this case, receptor binding and upregulation occur in the lymphatic system compartment during transport into the blood; therefore, upregulation of the receptor leads to IL-12 sequestration in the lymphatic system. Overall, both models are based on the principle that STAT4 activation in T-cells leads to upregulated IL-12 receptor expression, with the key difference being whether this leads to accelerated clearance or reduced bioavailability. As such, we correspondingly term our models as the accelerated-clearance model (**Equations 1-9, Figure 1A**) and the reduced-bioavailability model (**Equations 10-19, Figure 1B**).

The accelerated-clearance model predicts an apparent reduction in IL-12 half-life with subsequent doses.

To understand if the accelerated clearance model can capture trends of IL-12 desensitization in published clinical trial data, we fitted the model to three separate clinical PK datasets of repeated subcutaneous IL-12 injections with global optimization. The results are presented in **Figures 2A-B** (see also: **SI Text, Supplemental Tables S1-2**) and demonstrate that this model captures the relative magnitude of IL-12 desensitization, but the overall shape of time-course curves is

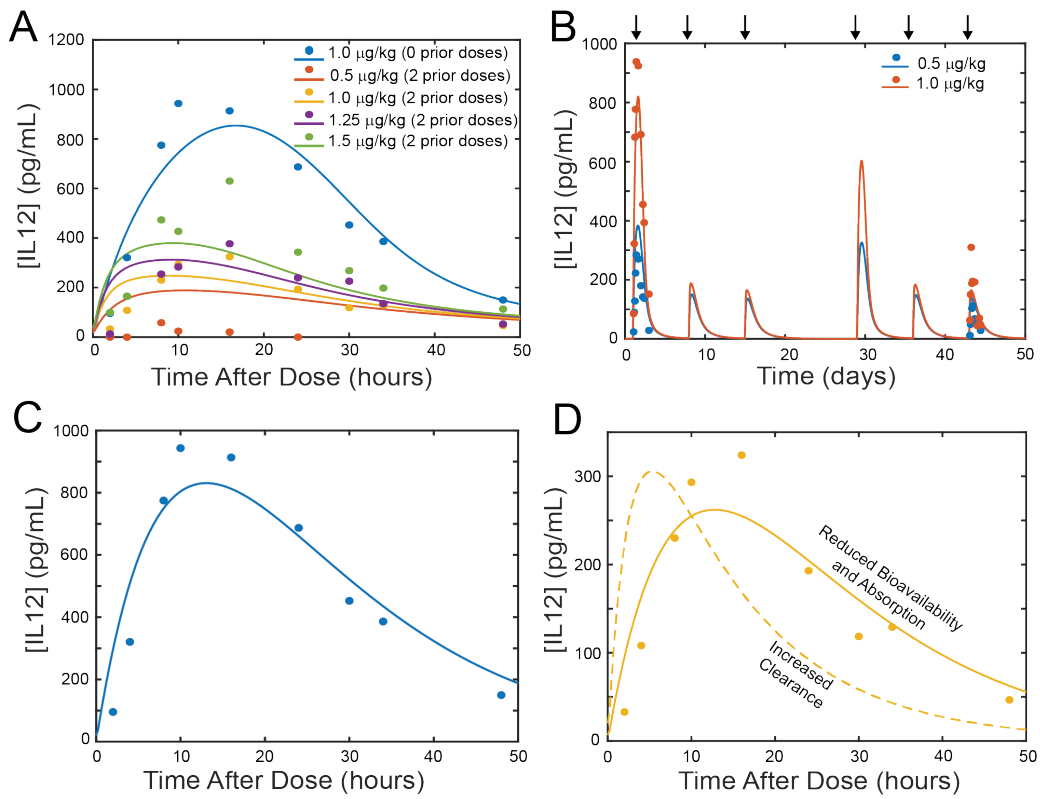

Figure 2: Accelerated-clearance model fitness to clinical trial data with and without feedback. A) Accelerated-clearance model fit to clinical trial data presented by Motzer et al. B) Accelerated-clearance model fit to clinical trial data presented by Rakhit et al. Black arrows represent dose administration C) Accelerated-clearance model fit to IL-12 time course data following 1.0 μg/kg administration with no prior doses from Motzer et al. D) Accelerated-clearance model refit to IL-12 time course data 1.0 μg/kg administration with two prior doses from Motzer et al. All model parameters other than bioavailability and absorption (solid line) or systemic clearance rate (dashed line) fixed to values in C).

177 inaccurate. More specifically, the model predicts that the increased IL-12 clearance from the blood
178 leads to an earlier time of maximum concentration and a reduced half-life. However, in contrast
179 with these predictions, the data from clinical trials suggests that neither maximal time nor half-life
180 changes significantly with repeated exposure to IL-12[13,14]. Therefore, we conclude that IL-12 PK
181 desensitization is unlikely to directly result from IL-12 upregulation in the blood. Accordingly,
182 the proposed mechanism in the accelerated-clearance model alone cannot account for IL-12 PK
183 desensitization.

184 To determine the shifts in the model parameter space associated with desensitization, we next
185 analyzed the accelerated-clearance model without feedback. To do this, we removed feedback
186 from the accelerated-clearance model by setting the feedback parameter α equal to zero (see
187 equation 12), and separately fit IL-12 PK data from patients with and without prior IL-12 exposure.
188 The data presented by Motzer and colleagues contains IL-12 serum concentrations at various time
189 points after 1.0 μg/kg doses with and without prior exposure to IL-12. To determine the shifts in
190 the PK parameter associated with prior exposure to IL-12, we first fit the dataset without prior
191 exposure to estimate the model parameters in the absence of desensitization (**Figure 2C**). Leaving
192 all other parameters fixed, we then fit the dataset with previous exposure only varying either the
193 IL-12 clearance rate (k_{CB}) or IL-12 bioavailability and absorption (J_{BS} and F). Manipulating IL-
194 12 clearance did not allow for the desensitized dataset to be captured with high fitness, but altering
195 bioavailability and absorption accurately fit both the magnitude of desensitization and the shape
196 of the data (**Figure 2D**). Ultimately, these results suggested that a mechanism related to the
197 bioavailability and absorption of IL-12 in the blood is more likely to contribute to IL-12 PK
198 desensitization.

199

The reduced bioavailability model accurately predicts IL-12 PK across all three clinical trials.

Next, we sought to determine whether our proposed mechanism influencing IL-12 bioavailability and transport into the blood can accurately fit IL-12 PK data reported in clinical trials. To this end, we fit the reduced-bioavailability model to all three clinical trials via global optimization. Optimization results illustrate that this model can fit these datasets accurately (**Figures 3A-B, Supplemental Tables S3-4**). Importantly, unlike the accelerated-clearance model, this model captures both the magnitude and overall shape of the datasets. The ability of the reduced-bioavailability model to fit all three datasets with different dose regiments supports its robustness.

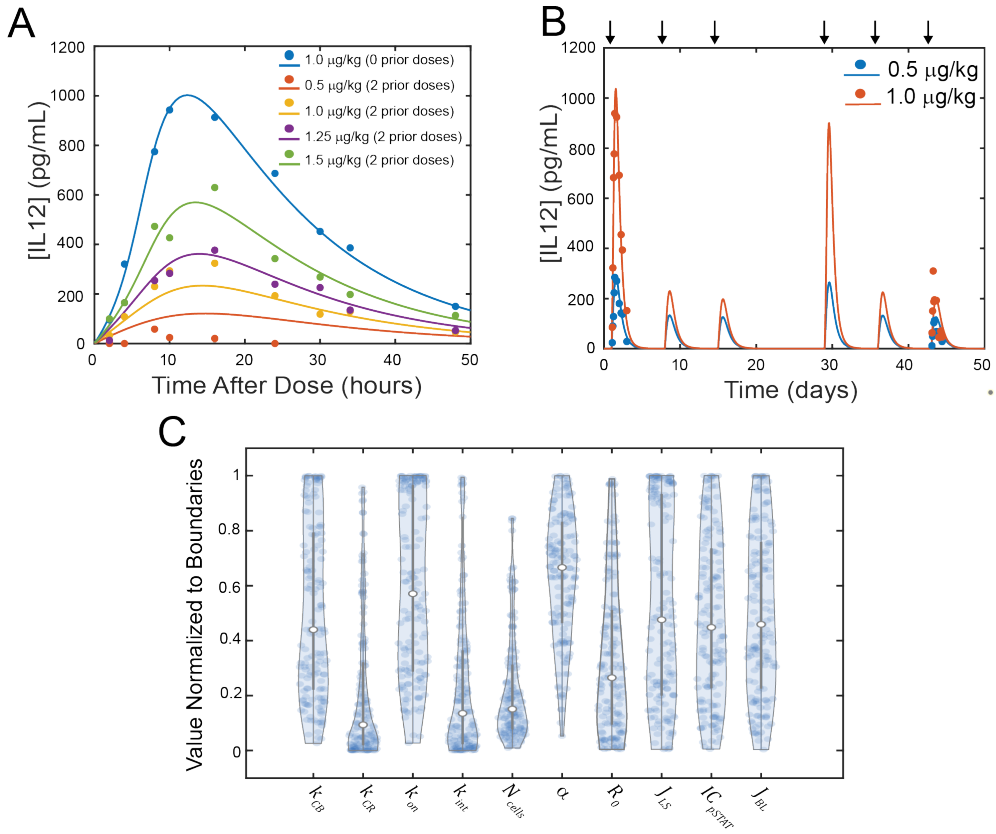

Figure 3: Reduced-bioavailability model fit to clinical trial data. A) Reduced-bioavailability model fit to clinical trial data presented by Motzer et al. after global optimization. B) Reduced-bioavailability model fit to clinical trial data presented by Rakhit et al. after global optimization. C) Distribution of generated ensemble fit to all three clinical trials following local optimization of randomly sampled parameter sets within boundaries (50 parameter sets per clinical trial).

208 As PK parameters often vary between patients[22], we sought to determine if our model can
209 accurately fit IL-12 PK data over a wide range of biologically relevant parameter values. An
210 ensemble of parameter sets was obtained by locally optimizing many sampled parameter sets to
211 each clinical trial. This method yields model parameter sets with slightly worse fitness to data
212 when compared to global optimization (**SI Text, Supplemental Figure S1**) but gives us a
213 distribution of parameter sets to analyze. Analysis of parameter distributions from all three fits
214 illustrates that model parameters are not tightly constrained and are widely distributed over the
215 optimization boundaries (**Figure 3C**). Furthermore, the distribution of parameter values does not
216 vary significantly based on the clinical trial used for fitting (**SI text, Supplemental Figure S2).**
217 These results illustrate that the prediction of IL-12 PK desensitization occurs over a large range of
218 parameter values and that the available data does not sufficiently restrict the PK parameters.

219 *Analysis of model behavior illustrates the effects of dosing regimen and model parameters on*
220 *desensitization.*

221 To gain insight into how the dosing regimen and model parameters influence the amount of IL-12
222 PK desensitization in the reduced bioavailability model, we simulated the reduced-bioavailability
223 model under various dosing conditions and parameter values to determine the effects on the
224 amount of desensitization predicted. For this analysis we use the parameters obtained via global
225 optimization to the data presented by Motzer and colleagues[13]. We first investigated the amount
226 of desensitization our model predicts following two consecutive doses of IL-12 with varying dose
227 amounts (**Figure 4A**) and time between doses (**Figure 4B**). Predictions illustrate that the extent
228 of desensitization increases with higher doses and doses that are closer in time. We hypothesized
229 that desensitization is mainly controlled by the concentration of receptor remaining in the
230 lymphatic system by the time of the next dose. A larger dose leads to increased STAT4 activation

and a more significant increase in receptor expression, and doses closer in proximity lead to less receptor clearance back to baseline before the next dose.

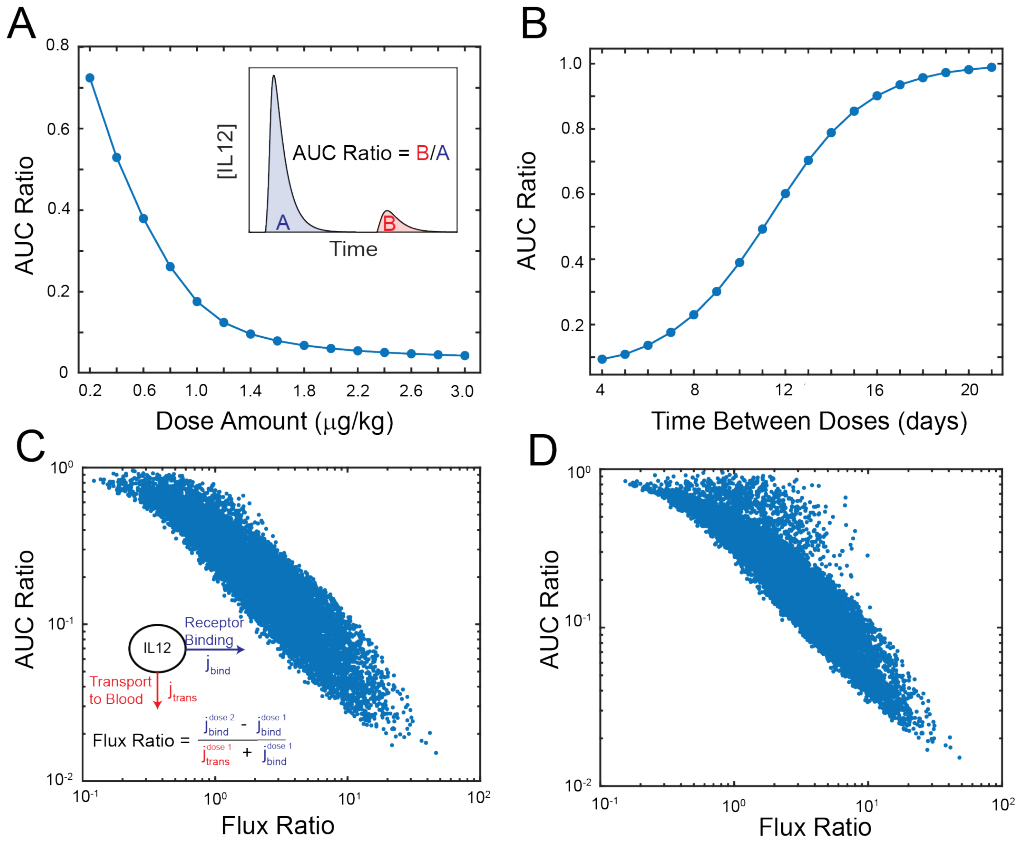

Figure 4: Analysis of model and dosing parameters influence on predicted amounts of desensitization. A) Predicted amount of desensitization after two consecutive IL-12 doses seven days apart at varying dose levels. Inset: visual representation of AUC ratio. B) Predicted amount of desensitization after two consecutive 1.0 μg/kg doses with varying time between doses. C) Relationship between predicted amount of desensitization based on numerically determined flux ratio. Inset: visual representation of flux ratio. D) Relationship between predicted amount of desensitization and analytically approximated flux ratio.

We next analyzed how variations in specific parameters related to receptor upregulation influence the amount of desensitization predicted. First, local sensitivity analyses were implemented for two and three consecutive doses of 0.5, 1.0, and 1.5 μg/kg, revealing which model parameters were most sensitive to the predicted amount of desensitization (**SI Text, Supplemental Figure S3**). The only model parameter with negligible impact on desensitization was k_{CB}, the clearance rate of IL-

238 12 from the blood. All other parameters had log gain sensitivities that were close to one in some
239 doses simulated. Of interest, parameters related to the amount of receptor initially (R_0, N_{cells}) and
240 the lifetime of receptor (k_{CR}, k_{int}) had log gain sensitivities greater than one at some dose levels.

241 To expand on the influence of the parameters related to receptor lifetime, initial receptor
242 concentrations, and feedback dynamics we generated an ensemble of 10,000 parameter sets
243 varying $k_{CR}, k_{int}, N_{cells}, \alpha, R_0,$ and IC_{pSTAT} between 50% and 150% of the optimized values
244 holding all other parameters constant. Each parameter set was simulated for two consecutive 1.0
245 μg/kg doses on days 1 and 8 of a 15-day cycle, and the amount of desensitization predicted was
246 quantified based on equation 24. Analysis of these simulations illustrated that the amount of
247 desensitization that occurs is correlated to the increase in binding flux at the time of the second
248 dose (t = τ) normalized by the total flux of IL-12 out of the lymphatic system at the time of the
249 first dose (t = 0), determined by equation 30. More specifically, we found that the value Ψ was
250 inversely correlated to the AUC ratio and, therefore, positively correlated with the extent of
251 desensitization predicted (**Figure 4C**)

$$\Psi = \frac{R(\tau) - k_{on}R(0)}{J_{BL} + k_{on}R(0)} \tag{30}$$

252 To gain deeper insight into the role specific parameters have on the amount of receptor remaining
253 at the time of the second dose and the amount of desensitization predicted, we derived an analytical
254 approximation for the concentration of receptor in the lymphatic system following a single dose
255 (**SI Text, Equations S41-S45**) This approximation of receptor concentrations is in reasonable
256 agreement with numerical simulations, especially at longer time points where the receptor
257 concentration is close to baseline levels (**SI Text, Supplemental Figure S4**). Using this

approximation to calculate the increase in receptor binding flux at the time of second dose based on equation 31, we obtain:

$$\Psi = \frac{k_{on}[e_1(\tau) + e_2(\tau) + e_3(\tau)]}{J_{BL} + k_{on}R(0)} \tag{31}$$

Here, the three exponential terms $e_1(t), e_2(t)$, and $e_3(t)$ are given by equations S42-S44 (see **SI Text**). When used to predict the magnitude of IL-12 desensitization that occurs, equation 31 yields results similar to those extracted from numerical simulations (**Figure 4D, SI Text, Supplemental Figure S5**). Our analytical expression illustrates how specific parameters influence the amount of desensitization predicted without numerical simulation. We see that terms in the numerator of ϕ will lead to a larger peak in receptor concentration, and vice versa for the denominator. Additionally, increases in the three exponential decay parameters, $J_{LS}, k_{int},$ and k_{CR}, lead to faster receptor clearance. If all three decay timescales are sufficiently short, upregulated receptor will clear by the time of the second dose and desensitization will not be predicted. Furthermore, we predict that multiple processes in our model contribute to the presence of desensitization, and that desensitization will be predicted over a variety of different parameter combinations. Generally, the requirement for desensitization in our model is that the upregulated of IL-12 receptor remains present when the next dose is administered. We show here that this behavior is not specific to a small subset of parameter values, supporting the robustness of our model to predict desensitization despite the inherent variability in our model parameters.

Simulation of local IL-12 delivery reveals potential strategies for limiting systemic exposure to IL-12 while maintaining desired local concentrations.

Next, we sought to explore the consequences of our proposed mechanism in designing IL-12 therapies for limiting systemic exposure to IL-12. As current interest in IL-12 therapy revolves

279 around local cytokine delivery via cell or gene therapy, we modified the reduced bioavailability
280 model to represent continuous local production of IL-12. These analyses are completed in the
281 context of intraperitoneal delivery but are generally applicable to local delivery of IL-12 in any
282 peripheral tissue. Before simulating continuous intraperitoneal administration of IL-12, we first
283 estimated the parameters describing IL-12 transport from the intraperitoneal space to the blood by
284 fitting our model to clinical trial data presented by Lenzi et al.[23] modified to represent
285 intraperitoneal injection of IL-12. Our model was able to accurately fit both the intraperitoneal
286 and serum IL-12 concentrations (**Supplemental Figure S6**), giving us confidence in the estimated
287 transport parameters. Additionally, a standard PK model is unable to fit this data, further
288 supporting the relevance of our model. Since this dataset only consisted of a single intraperitoneal
289 infusion of IL-12, we used the transport parameters estimated from the Lenzi et al. data[23] and
290 parameters to characterize receptor-upregulation feedback estimated from our fits in earlier
291 sections.

292 Using the estimated parameters for intraperitoneal transport of IL-12, we modified the reduced
293 bioavailability model to represent continuous, local delivery of IL-12 in the peritoneal cavity. The
294 modified version of the accelerated-clearance model consists of the same ordinary differential
295 equations as previously outlined, modified to represent the administration of IL-12 to the
296 peritoneal cavity with a given production/injection rate. The complete model equations and
297 parameter values used for these analyses are located in the supplemental text.

298 We first predicted intraperitoneal and serum concentrations of IL-12 following continuous
299 intraperitoneal delivery according to three different production profiles: 1) constant production,
300 2) step-wise production, and 3) linearly increasing production (**Figure 5A**). All three production

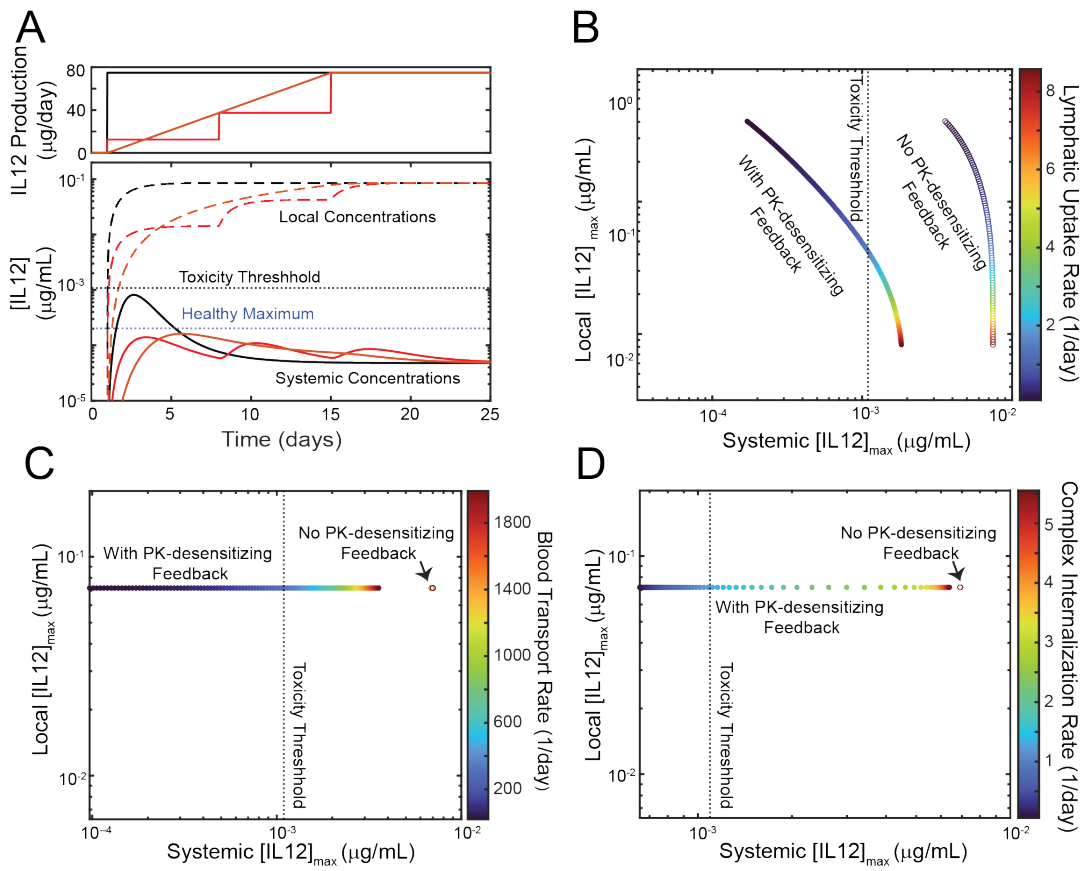

Figure 5: Model predictions of strategies for mitigating systemic IL-12 exposure following continuous local delivery. A) Prediction of continuous, intraperitoneal IL-12 delivery according to three different production rate profiles: constant production (black lines), step-wise production (red lines), and linearly increasing production (orange lines). Healthy IL-12 serum concentration taken from Derin et al.[24] B-D) Effects of various IL-12 related parameters on maximum concentrations in the local environment and in the blood. B) Effects of manipulating lymphatic uptake. C) Effects of limiting transport into the blood from the lymphatic system. C) Effects of limiting internalization of IL-12:IL-12 receptor complex.

profiles were designed to reach an equivalent concentration of IL-12 in the intraperitoneal space at steady state. Importantly, our model predicts serum IL-12 concentrations far above normal levels[24] following the constant production profile that does not occur in either of the dynamic dosing strategies. Additionally, the concentration of IL-12 in the intraperitoneal space at long times is indeed equivalent for all three strategies. These results suggest that systemic exposure to

306 IL-12 may be avoided following local delivery by utilizing dosing strategies that slowly reach the
307 desired production rate for local concentrations rather than immediately starting at that level.

308 In addition to analyzing the predicted effects of dynamic dosing strategies, we used our model to
309 identify potential protein engineering approaches for limiting systemic exposure. Based on our
310 simulations, strategies modifying IL-12 to limit uptake into the lymphatic system from the local
311 environment (**Figure 5B**), limit uptake into the blood from the lymphatic system (**Figure 5C**), or
312 limit internalization of IL-12:IL-12 receptor complex (**Figure 5D**) were predicted to have profound
313 effects due to our mechanism. We found that these aspects of IL-12 could be manipulated such
314 that the systemic exposure to IL-12 is reduced, and the concentrations in the local environment are
315 either increased or unchanged. These strategies are a direct result of IL-12 PK desensitization;
316 without our mechanism, they are not predicted to be effective. Ultimately, these results illustrate
317 how our proposed mechanism for IL-12 desensitization can be leveraged to identify strategies for
318 limiting systemic exposure to IL-12 treatment.

319 **Discussion**

320 Here, we employ a modeling approach to validate proposed mechanisms for IL-12 PK
321 desensitization. Two models of IL-12 PK containing feedback mechanisms causing increased
322 clearance or reduced bioavailability following repeated doses of IL-12 were developed. The
323 accelerated-clearance model failed to capture IL-12 PK accurately, whereas the reduced-
324 bioavailability model accurately fit IL-12 PK across three separate clinical trials. Ultimately, our
325 results allowed us to develop a model that can accurately predict IL-12 PK desensitization, which
326 is not currently available to the best of our knowledge.

327 The molecular mechanism we propose for IL-12 PK desensitization is that IL-12 stimulation of T-
328 cells in the lymphatic system leads to increased expression of the IL-12 receptor and IL-12
329 sequestration during transport into the blood. This mechanism is based on the observation in
330 literature that IL-12 activation of STAT4 in T-cells leads to increased IL-12 receptor expression in
331 both *in vitro* and *in vivo* experiments[17,19]. These studies illustrated the presence of this feedback
332 loop; however, its specific effects on IL-12 desensitization have yet to be fully elucidated. Our
333 results provide quantitative justification for how upregulation of IL-12 receptor affects IL-12 PK.
334 While this effect is likely seen in T-cells throughout the entire body, we hypothesize in our model
335 that this mechanism is most important in the lymphatic system due to the large number of T-cells
336 and the role in IL-12 transport to the blood. Incorporation of this molecular mechanism into our
337 model allowed for IL-12 PK to be accurately fit in three separate clinical trials, supporting our
338 hypothesis. Furthermore, analysis of parameter distributions illustrated that desensitization is
339 predicted over a wide range of biologically relevant parameter values, supporting the robustness
340 of this mechanism.

341 We next sought to explore the implications of our proposed mechanism on the design of IL-12
342 therapies. The development of IL-12 therapies today focuses on local delivery of IL-12 through
343 gene or cell-based therapies[7,8,11,16,25,26]. These technologies are designed to maintain high levels
344 of IL-12 near the tumor while limiting systemic IL-12 exposure. Importantly, technologies where
345 significant IL-12 exposure occurs cause severe toxicities, limiting the therapeutic window of
346 treatment[26]. Based on these observations, we used our model to identify potential strategies
347 leveraging IL-12 PK desensitization to maintain low levels of IL-12 exposure. We found that
348 designing IL-12 therapies to begin with lower production rates and slowly increase until reaching
349 the desired dose can prevent initial spikes in IL-12 exposure. Furthermore, we identified several

350 protein engineering approaches that can be utilized to maximize concentrations in the local
351 environment while limiting serum exposure to IL-12.

352 The molecular mechanism we suggest for IL-12 PK desensitization provides an example of how
353 regulation of a biologic's target can influence the bioavailability of the therapeutic. Unlike small
354 molecules, biologics are known to have complex PK due to their large molecular weights, strong
355 binding to their targets, and connection between PK and PD[27]. The influence of target binding on
356 biologic PK is known as target-mediated drug disposition (TMDD)[28]. More specifically, TMDD
357 involves target-mediated clearance of the biologic, and since the abundance of targets is finite
358 these effects become dose-dependent. Additionally, cases have been identified where a biologic
359 upregulates the abundance of its target, leading to an increase in clearance[28]. For example,
360 pegfilgrastim is a colony-stimulating factor targeting neutrophils, and activity leads to neutrophil
361 proliferation. As a result, pegfilgrastim stimulation leads to increased target abundance and an
362 increase of drug clearance[29]. While these effects are typically related to increased clearance of a
363 biologic, our results provide a quantitative explanation for how target upregulation can also affect
364 bioavailability. Despite our focus on IL-12, our results provide insight into complex PK of other
365 biologics. In cases where a biologic's target is highly abundant in the lymphatic system and
366 upregulated by the biologic's action, we show that the bioavailability of the therapeutic can
367 decrease with repeated dosing.

368 **Study Highlights**

369 What is the current knowledge on this topic?

370 IL-12 desensitization was observed in the earliest clinical trials investigating IL-12
371 immunotherapy, and several studies have linked the phenomenon to treatment efficacy and

372 tolerability. Mechanisms have been hypothesized in literature, but none have been validated
373 quantitatively.

374 What question did this study address?

375 What is the desensitization mechanism capable of correctly predicting IL-12 pharmacokinetics
376 over repeated doses, and what are the therapeutic consequences of that mechanism?

377 What does this study add to our knowledge?

378 Our results illustrate that IL-12 PK desensitization is likely to be a result of decreased
379 bioavailability after repeated exposure to IL-12 rather than increased systemic clearance. We
380 propose a molecular mechanism for this model based on the upregulation of IL-12 receptor on T-
381 cells in the lymphatic system. Our model provides a framework capable of predicting IL-12
382 pharmacokinetics which, to the best of our knowledge, does not currently exist.

383 How might this change clinical pharmacology or translational science?

384 Pharmacokinetic modeling is essential in predicting the behavior of therapeutics in humans. We
385 provide a tool for predicting IL-12 pharmacokinetics, which will undoubtedly aid in the
386 development of IL-12 based therapies.

387 **Author Contributions**

388 J.D., O.A.I., and O.V. wrote the manuscript; J.D. and O.A.I. designed the research; J.D
389 performed the research; J.D. and O.A.I. analyzed the data.

390

391 **References**

392 1. Cirella A, Luri-Rey C, Di Trani CA, et al. Novel strategies exploiting interleukin-12 in
393 cancer immunotherapy. *Pharmacology & Therapeutics*. 2022;239:108189.
394 doi:10.1016/j.pharmthera.2022.108189

395 2. Berger A. Th1 and Th2 responses: what are they? *BMJ*. 2000;321(7258):424.

396 3. Gately MK, Renzetti LM, Magram J, et al. THE INTERLEUKIN-12/INTERLEUKIN-12-
397 RECEPTOR SYSTEM: Role in Normal and Pathologic Immune Responses. *Annual Review*
398 *of Immunology*. 1998;16(1):495-521. doi:10.1146/annurev.immunol.16.1.495

399 4. Athie-Morales V, Smits HH, Cantrell DA, Hilkens CMU. Sustained IL-12 Signaling Is
400 Required for Th1 Development 1. *The Journal of Immunology*. 2004;172(1):61-69.
401 doi:10.4049/jimmunol.172.1.61

402 5. Atkins MB, Robertson MJ, Gordon M, et al. Phase I evaluation of intravenous recombinant
403 human interleukin 12 in patients with advanced malignancies. *Clin Cancer Res*.
404 1997;3(3):409-417.

405 6. Leonard JP, Sherman ML, Fisher GL, et al. Effects of Single-Dose Interleukin-12 Exposure
406 on Interleukin-12–Associated Toxicity and Interferon-γ Production. *Blood*. 1997;90(7):2541-
407 2548. doi:10.1182/blood.V90.7.2541

408 7. Algazi AP, Twitty CG, Tsai KK, et al. Phase II Trial of IL-12 Plasmid Transfection and PD-1
409 Blockade in Immunologically Quiescent Melanoma. *Clinical Cancer Research*.
410 2020;26(12):2827-2837. doi:10.1158/1078-0432.CCR-19-2217

411 8. Algazi A, Bhatia S, Agarwala S, et al. Intratumoral delivery of tavokinogene telseplasmid
412 yields systemic immune responses in metastatic melanoma patients. *Ann Oncol*.
413 2020;31(4):532-540. doi:10.1016/j.annonc.2019.12.008

414 9. Bajetta E, Del Vecchio M, Mortarini R, et al. Pilot study of subcutaneous recombinant
415 human interleukin 12 in metastatic melanoma. *Clinical Cancer Research*. 1998;4(1):75-85.

416 10. Bekaii-Saab TS, Roda JM, Guenterberg KD, et al. A phase I trial of paclitaxel and
417 trastuzumab in combination with interleukin-12 in patients with HER2/neu-expressing
418 malignancies. *Molecular Cancer Therapeutics*. 2009;8(11):2983-2991. doi:10.1158/1535-
419 7163.MCT-09-0820

420 11. Bhatia S, Longino NV, Miller NJ, et al. Intratumoral Delivery of Plasmid IL12 Via
421 Electroporation Leads to Regression of Injected and Noninjected Tumors in Merkel Cell
422 Carcinoma. *Clinical Cancer Research*. 2020;26(3):598-607. doi:10.1158/1078-0432.CCR-
423 19-0972

424 12. Gollob JA, Mier JW, Veenstra K, et al. Phase I Trial of Twice-Weekly Intravenous
425 Interleukin 12 in Patients with Metastatic Renal Cell Cancer or Malignant Melanoma: Ability

426 to Maintain IFN-γ Induction Is Associated with Clinical Response1. *Clinical Cancer*
427 *Research*. 2000;6(5):1678-1692.

428 13. Motzer RJ, Rakhit A, Schwartz LH, et al. Phase I trial of subcutaneous recombinant human
429 interleukin-12 in patients with advanced renal cell carcinoma. *Clinical Cancer Research*.
430 1998;4(5):1183-1191.

431 14. Portielje JEA, Kruit WHJ, Schuler M, et al. Phase I Study of Subcutaneously Administered
432 Recombinant Human Interleukin 12 in Patients with Advanced Renal Cell Cancer. *Clinical*
433 *Cancer Research*. 1999;5(12):3983-3989.

434 15. Portielje JEA, Lamers CHJ, Kruit WHJ, et al. Repeated Administrations of Interleukin (IL)-
435 12 Are Associated with Persistently Elevated Plasma Levels of IL-10 and Declining IFN-γ,
436 Tumor Necrosis Factor-α, IL-6, and IL-8 Responses. *Clinical Cancer Research*.
437 2003;9(1):76-83.

438 16. Barton KN, Siddiqui F, Pompa R, et al. Phase I trial of oncolytic adenovirus-mediated
439 cytotoxic and interleukin-12 gene therapy for the treatment of metastatic pancreatic cancer.
440 *Molecular Therapy - Oncolytics*. 2021;20:94-104. doi:10.1016/j.omto.2020.11.006

441 17. Rakhit A, Yeon MM, Ferrante J, et al. Down-regulation of the pharmacokinetic-
442 pharmacodynamic response to interleukin-12 during long-term administration to patients
443 with renal cell carcinoma and evaluation of the mechanism of this "adaptive response" in
444 mice. *Clinical Pharmacology & Therapeutics*. 1999;65(6):615-629. doi:10.1016/S0009-
445 9236(99)90083-8

446 18. Coughlin CM, Wysocka M, Trinchieri G, Lee WMF. The Effect of Interleukin 12
447 Desensitization on the Antitumor Efficacy of Recombinant Interleukin 121. *Cancer*
448 *Research*. 1997;57(12):2460-2467.

449 19. Becskei A, Grusby MJ. Contribution of IL-12R mediated feedback loop to Th1 cell
450 differentiation. *FEBS Letters*. 2007;581(27):5199-5206. doi:10.1016/j.febslet.2007.10.007

451 20. Wang KS, Zorn E, Ritz J. Specific down-regulation of interleukin-12 signaling through
452 induction of phospho-STAT4 protein degradation. *Blood*. 2001;97(12):3860-3866.
453 doi:10.1182/blood.V97.12.3860

454 21. Martin JP, Rasor BJ, DeBonis J, et al. A dynamic kinetic model captures cell-free metabolism
455 for improved butanol production. *Metabolic Engineering*. 2023;76:133-145.
456 doi:10.1016/j.ymben.2023.01.009

457 22. Bensalem A, Ternant D. Pharmacokinetic Variability of Therapeutic Antibodies in Humans:
458 A Comprehensive Review of Population Pharmacokinetic Modeling Publications. *Clin*
459 *Pharmacokinet*. 2020;59(7):857-874. doi:10.1007/s40262-020-00874-2

460 23. Lenzi R, Rosenblum M, Verschraegen C, et al. Phase I Study of Intraperitoneal Recombinant
461 Human Interleukin 12 in Patients with Müllerian Carcinoma, Gastrointestinal Primary
462 Malignancies, and Mesothelioma1. *Clinical Cancer Research*. 2002;8(12):3686-3695.

463 24. Derin D, Soydinc HO, Guney N, et al. Serum IL-8 and IL-12 levels in breast cancer. *Medical*
464 *Oncology*. 2007;24(2):163-168. doi:10.1007/BF02698035

465 25. Greaney SK, Algazi AP, Tsai KK, et al. Intratumoral Plasmid IL12 Electroporation Therapy
466 in Patients with Advanced Melanoma Induces Systemic and Intratumoral T-cell Responses.
467 *Cancer Immunology Research*. 2020;8(2):246-254. doi:10.1158/2326-6066.CIR-19-0359

468 26. Zhang L, Morgan RA, Beane JD, et al. Tumor-Infiltrating Lymphocytes Genetically
469 Engineered with an Inducible Gene Encoding Interleukin-12 for the Immunotherapy of
470 Metastatic Melanoma. *Clinical Cancer Research*. 2015;21(10):2278-2288.
471 doi:10.1158/1078-0432.CCR-14-2085

472 27. Shi S. Biologics: An Update and Challenge of Their Pharmacokinetics. *Current Drug*
473 *Metabolism*. 2014;15(3):271-290.

474 28. An G. Concept of Pharmacologic Target-Mediated Drug Disposition in Large-Molecule and
475 Small-Molecule Compounds. *The Journal of Clinical Pharmacology*. 2020;60(2):149-163.
476 doi:10.1002/jcph.1545

477 29. Roskos LK, Lum P, Lockbaum P, Schwab G, Yang BB. Pharmacokinetic/Pharmacodynamic
478 Modeling of Pegfilgrastim in Healthy Subjects. *The Journal of Clinical Pharmacology*.
479 2006;46(7):747-757. doi:10.1177/0091270006288731

480

481

482 **Figure Legends**

483 **Figure 1: Schematics detailed two models developed in this investigation.** A) Schematic of
484 accelerated-clearance model. B) Schematic of reduced-bioavailability model.

485 **Figure 2: Accelerated-clearance model fitness to clinical trial data with and without**
486 **feedback**. A) Accelerated-clearance model fit to clinical trial data presented by Motzer et al. B)
487 Accelerated-clearance model fit to clinical trial data presented by Rakhit et al. Black arrows
488 represent dose administration C) Accelerated-clearance model fit to IL-12 time course data
489 following 1.0 μg/kg administration with no prior doses from Motzer et al. D) Accelerated-
490 clearance model refit to IL-12 time course data 1.0 μg/kg administration with two prior doses
491 from Motzer et al. All model parameters other than bioavailability and absorption (solid line) or
492 systemic clearance rate (dashed line) fixed to values in C).

493 **Figure 3: Reduced-bioavailability model fit to clinical trial data**. A) Reduced-bioavailability
494 model fit to clinical trial data presented by Motzer et al. after global optimization. B) Reduced-
495 bioavailability model fit to clinical trial data presented by Rakhit et al. after global optimization.
496 C) Distribution of generated ensemble fit to all three clinical trials following local optimization
497 of randomly sampled parameter sets within boundaries (50 parameter sets per clinical trial).

498 **Figure 4: Analysis of model and dosing parameters influence on predicted amounts of**
499 **desensitization.** A) Predicted amount of desensitization after two consecutive IL-12 doses seven
500 days apart at varying dose levels. Inset: visual representation of AUC ratio. B) Predicted amount
501 of desensitization after two consecutive 1.0 μg/kg doses with varying time between doses. C)
502 Relationship between predicted amount of desensitization based on numerically determined flux

503 ratio. Inset: visual representation of flux ratio. D) Relationship between predicted amount of
504 desensitization and analytically approximated flux ratio.

505 **Figure 5: Model predictions of strategies for mitigating systemic IL-12 exposure following**
506 **continuous local delivery.** A) Prediction of continuous, intraperitoneal IL-12 delivery
507 according to three different production rate profiles: constant production (black lines), step-wise
508 production (red lines), and linearly increasing production (orange lines). Healthy IL-12 serum
509 concentration taken from Derin et al.[24] B-D) Effects of various IL-12 related parameters on
510 maximum concentrations in the local environment and in the blood. B) Effects of manipulating
511 lymphatic uptake. C) Effects of limiting transport into the blood from the lymphatic system. C)
512 Effects of limiting internalization of IL-12:IL-12 receptor complex.

SUPPLEMENTARY INFORMATION FOR

Uncovering the Interleukin-12 Pharmacokinetic Desensitization and Its Consequences with Mathematical Modeling

Jonathon DeBonis, Omid Veiseh, and Oleg Igoshin

Oleg Igoshin

Email: igoshin@rice.edu

This PDF file includes:

Supplementary Tables S1 to S7	S2
Supplementary Figures S1 to S8	S8
Supplementary Text	S13
Supplementary References	S25

Supplemental Table S1: Reported IL-12 C_{max}, AUC, and t_{max} by Portielje et al. following repeated s.c. injections compared to accelerated-clearance model predictions after global optimization. Predicted values are reported to two significant digits.

Dose Information	Predicted C_{max}	Reported C_{max}	Predicted AUC	Reported AUC	Predicted t_{max}	Reported t_{max}
0.5 $\mu g/kg$, dose 1	430 pg/mL	362 (214) pg/mL	8,200 pg*h/mL	7,400 (5,400) pg*h/mL	5.1 h	9.7 (5) h
0.5 $\mu g/kg$, dose 7	250 pg/mL	255 (200) pg/mL	4,000 pg*h/mL	3,300 (1,600) pg*h/mL	2.8 h	9.5 (2.2) h
1.0 $\mu g/kg$, dose 1	1000 pg/mL	1131 (1051) pg/mL	22,000 pg*h/mL	31,800 (22,300) pg*h/mL	8.4 h	17 (7) h
1.0 $\mu g/kg$, dose 7	360 pg/mL	376 (49) pg/mL	5,600 pg*h/mL	6,000 (2,400) pg*h/mL	2.3 h	4 (0) h

*Values in () are reported standard deviation.

Supplemental Table S2: Accelerated-clearance model parameter values following global optimization to three clinical trials individually. Values are reported to two significant digits.

Parameter	Value fit to Motzer data	Value fit to Rakhit data	Value fit to Portielje data
k_{CB} (days^{-1})	0.80	0.80	0.80
k_{CR} (days^{-1})	0.75	0.46	0.46
k_{on}(mL pmol^{-1}days^{-1})	200	200	210
k_{int}(days^{-1})	0.49	0.49	0.46
α (days^{-1})	3.5e-6	3.9e-6	2.8e-6
F (unitless)	0.83	0.41	0.60
J_{BS} (days^{-1})	0.25	0.27	1.2
R_0 (pmol/cell)	1.8e-9	1.7e-9	6.7e-9
N_{cells}(cells)	4.2e10	4.2e10	5.2e10
IC_{pSTAT} (#/cell)	6.6e5	8.2e5	1.8e6

Supplemental Table S3: Reported IL-12 C_{max}, AUC, and t_{max} by Portielje et al. following repeated s.c. injections compared to reduced-bioavailability model predictions after global optimization. Predicted values are reported to two significant digits.

Dose Information	Predicted C_{max}	Reported C_{max}	Predicted AUC	Reported AUC	Predicted t_{max}	Reported t_{max}
0.5 μg/kg, dose 1	330 pg/mL	362 (214) pg/mL	7,400 pg*h/mL	7,400 (5,400) pg*h/mL	10 h	9.7 (5) h
0.5 μg/kg, dose 7	170 pg/mL	255 (200) pg/mL	4,100 pg*h/mL	3,300 (1,600) pg*h/mL	10 h	9.5 (2.2) h
1.0 μg/kg, dose 1	1,300 pg/mL	1131 (1051) pg/mL	26,000 pg*h/mL	31,800 (22,300) pg*h/mL	9.8 h	17 (7) h
1.0 μg/kg, dose 7	290 pg/mL	376 (49) pg/mL	6,800 pg*h/mL	6,000 (2.4) pg*h/mL	10 h	4 (0) h

*Values in () are reported standard deviation.

Supplemental Table S4: Reduced-bioavailability model parameter values following global optimization to three clinical trials individually. Values are reported to two significant digits.

Parameter	Value fit to Motzer data	Value fit to Rakhit data	Value fit to Portielje data
$k_{CB}(\text{days}^{-1})$	1.6	2.4	2.4
$k_{CR}(\text{days}^{-1})$	0.46	0.50	1.7
$k_{on}(\text{mL pmol}^{-1}\text{days}^{-1})$	200	200	200
$k_{int}(\text{days}^{-1})$	0.56	0.59	0.66
$N_{cells}(\text{cells})$	3.8e10	3.3e10	1.7e11
$\alpha(\text{pmol cells}^{-1}\text{days}^{-1})$	5.0e-6	3.1e-6	4.4e-6
R_0 (pmol cells^{-1})	5.6e-9	5.5e-9	1.8e-9
J_{LS} (days^{-1})	1.6	1.2	2.9
J_{BL} (days^{-1})	70	130	150
IC_{pstat} (# cells^{-1})	1.4e6	9.8e5	1.8e6

Supplemental Table S5: Reported IL-12 C_{max}, AUC, and t_{max} by Portielje et al. following repeated s.c. injections compared to reduced-bioavailability model predictions after ensemble local optimization. Predicted values are reported to two significant digits.

Dose Information	Predicted C_{max}	Reported C_{max}	Predicted AUC	Reported AUC	Predicted t_{max}	Reported t_{max}
0.5 μg/kg, dose 1	350 (30) pg/mL	362 (214) pg/mL	8,700 (570) pg*h/mL	7,400 (5,400) pg*h/mL	9.6 (1.1) h	9.7 (5) h
0.5 μg/kg, dose 7	170 (15) pg/mL	255 (200) pg/mL	4,500 (180) pg*h/mL	3,300 (1,600) pg*h/mL	9.7 (0.86) h	9.5 (2.2) h
1.0 μg/kg, dose 1	940 (190) pg/mL	1131 (1051) pg/mL	21,000 (4,200) pg*h/mL	31,800 (22,300) pg*h/mL	9.3 (1.1) h	17 (7) h
1.0 μg/kg, dose 7	240 (20) pg/mL	376 (49) pg/mL	6,300 (290) pg*h/mL	6,000 (2,400) pg*h/mL	9.8 (0.94) h	4 (0) h

*Values in () are reported standard deviation.

Supplemental Table S6: Accelerated clearance model parameter information.

Parameter	Meaning	Optimization Range/Default Value	Source
k_{CB} (days^{-1})	IL-12 first order clearance rate from blood.	0.79 – 2.4	Reported half-life values in clinical trials (Motzer et al.[1], Rakhit et al.[2], Portielje et al.[3])
k_{CR} (days^{-1})	IL-12 receptor unbound internalization rate	0.46 – 1.1	Literature estimate unavailable, estimated based on half life between 10 and 36 hours.
k_{on}(mL pmol^{-1}days^{-1})	IL-12 IL-12 receptor association rate.	1.5 – 210	Chizzonite et al.[4], adjusted to have high binding rate for improved fit to data.

k_{int}(days^{-1})	IL-12 receptor bound internalization rate.	0.46 – 1.1	Literature estimate unavailable, estimated based on half life between 10 and 36 hours.
α (days^{-1})	Linear feedback coefficient for receptor upregulation model.	0.1 – 10	Estimated, given large range.
F (unitless)	Absolute bioavailability, fraction of administered IL-12 reaching blood.	0.010 – 1.0	Estimated, given range of reasonable values.
J_{BS} (days^{-1})	First order transport rate for IL-12 to the blood.	1.0e-4 – 5.0	Estimated, given large range.
R_0 (pmol mL^{-1})	Initial concentration of IL-12 receptor in blood.	0.0026 – 0.023	Estimated based on blood T-cell count (Sender et al.[5]) and reported binding sites per cell (Chizzonite et al.[4])
$IL12_{S,0}$ (pmol mL^{-1})	Initial concentration of IL-12 in the subcutaneous space.	n/a	Determined according to equation S1.1
k_{DG} (days^{-1})	First order degradation rate of IL-12 in the blood.	n/a	Determined according to equation S1.3
V_S (mL)	Volume of injection in subcutaneous space.	n/a	Based on volume of injection for clinical trials. Assumed to be 1 mL if not specified
V_B (mL)	Volume of the blood.	5100	Assumed as average human blood volume.
D(pmol)	Dose amount.	n/a	Given based on dose information.

Supplemental Table S7: Reduced-bioavailability model parameter information.

Parameter	Meaning	Optimization Range/Default Value	Sources
$J_{LS}(\text{days}^{-1})$	First order IL-12 transport rate from subcutaneous space to lymphatic system.	0.79 – 2.4	Milewski et al.[6]
$F(\text{unitless})$	Absolute bioavailability, fraction of IL-12 reaching lymphatic system.	1	Assumed to be one to isolate bioavailability mechanism.
k_{on} $(\text{mL pmol}^{-1}\text{days}^{-1})$	IL-12:IL-12 receptor association rate.	1.5 – 210	Chizzonite et al.[4], adjusted to have high binding rate for improved fit to data.
J_{BL} (days^{-1})	First order IL-12 transport rate from lymphatic system to blood.	4.3 – 430	Bounds centered around value reported by Varkhede et al.[7]
k_{CB} (days^{-1})	First order IL-12 clearance rate from blood.	0.79 – 2.4	Reported half-life values in clinical trials (Motzer et al.[1], Rakhit et al.[2], Portielje et al.[3])
$N_{cells}(\text{cells})$	Number of IL-12R+ T-cells in the lymphatic system	1.0e9 – 5.0e11	Sender et al.
k_{CR} (days^{-1})	IL-12 receptor unbound internalization rate.	0.46– 1.7	Literature estimate unavailable, estimated based on half life between 10 and 36 hours.
$\alpha(\text{pmol cells}^{-1}\text{days}^{-1})$	Linear feedback coefficient.	1.0e-8 – 1.0e-5	Estimated, given large range.
$R_0(\text{pmol cells}^{-1})$	Initial amount of receptor per T-cell in lymphatic system.	1.7e-9 – 1.5e-8	Chizzonite et al[4].
$IC_{pSTAT}(\#\ \text{cells}^{-1})$	Complex formation required for 50% maximum STAT4 activation.	9.1e2 – 1.8e6	Estimated, given large range.

k_{int} (days^{-1})	IL-12 receptor bound internalization rate.	0.46 – 1.7	Literature estimate unavailable, estimated based on half life between 10 and 36 hours.
V_S (mL)	Volume of injection in subcutaneous space.	Variable based on clinical trial.	Based on volume of injection for clinical trials. Assumed to be 1 mL if not specified
V_L (mL)	Volume of lymphatic system IL-12 enters in transport to blood.	33	Varkhede et al.[7]
V_B (mL)	Volume of blood.	5100	Average human blood volume.
k_R(pmol cells^{-1}days^{-1})	Basal receptor production rate.	n/a	Calculated by equation S2.7
k_{DG}(days^{-1})	First order degradation rate of IL-12 in the subcutaneous space.	n/a	Calculated by equation S2.2
$IL12_{S,0}$ (pmol mL^{-1})	Initial concentration of IL-12 in the subcutaneous space.	n/a	Calculated by equation S2.3
D(pmol)	Dose of IL-12 administered	Variable based on clinical trial.	Based on clinical trial information.

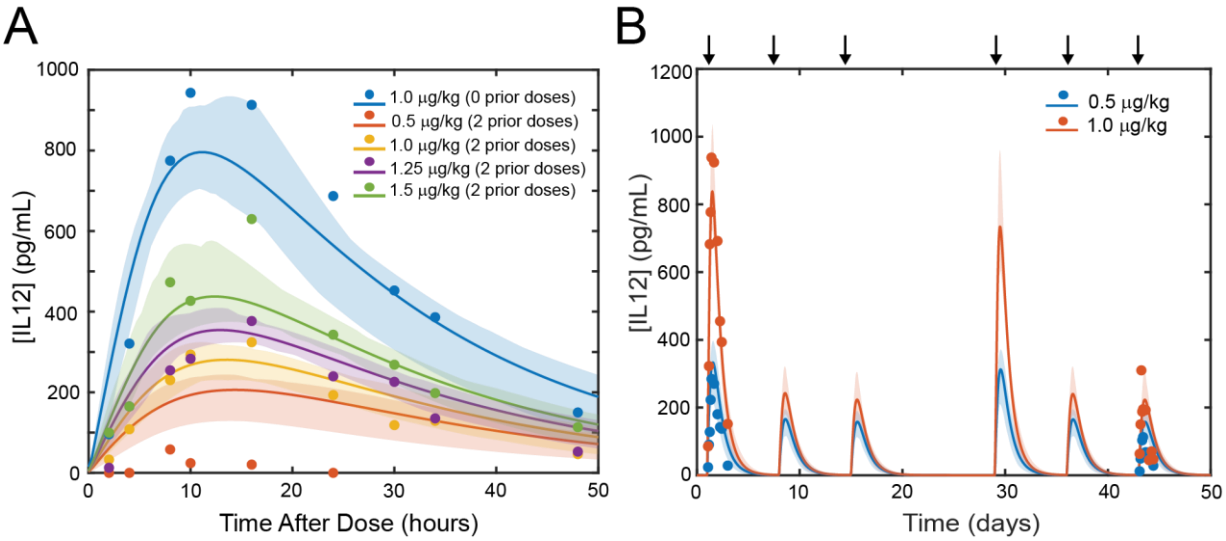

Supplemental Figure S1: Reduced bioavailability model fitness to clinical trial data following ensemble-based optimization. A) Model predictions fit to clinical trial data presented by Motzer et al.[1]. B) Model predictions fit to clinical trial data presented by Rakhit et al.[2]. Solid lines: mean predicted concentrations. Shaded area: raw 95% confidence interval.

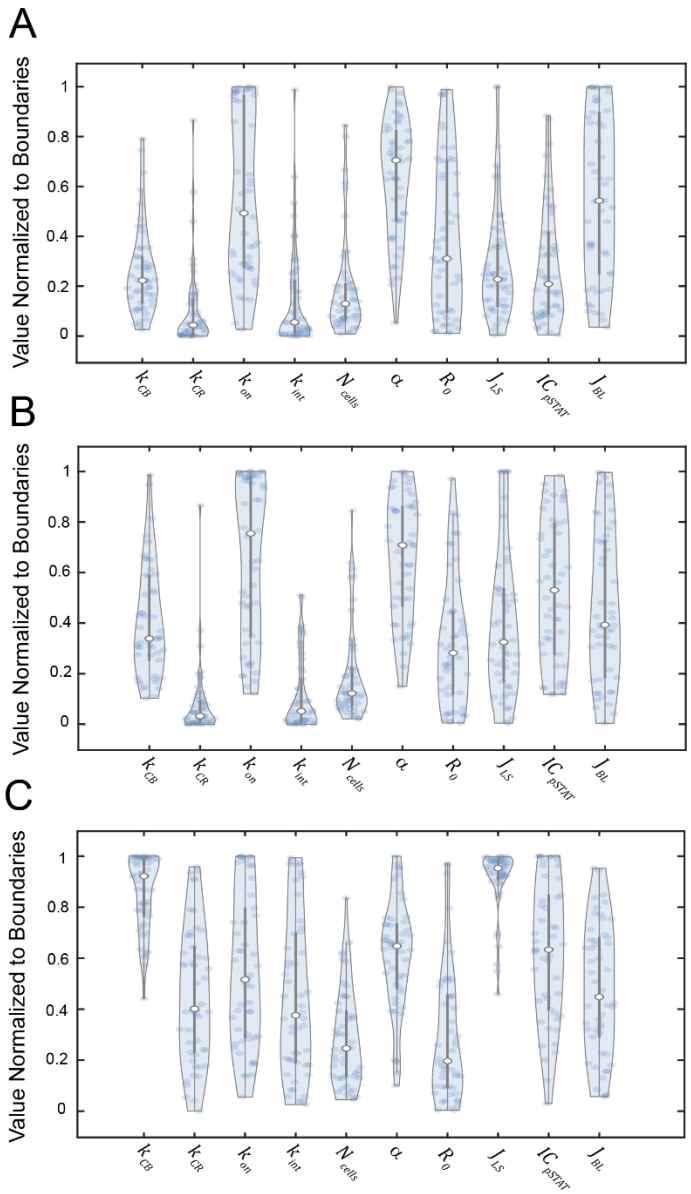

Supplemental Figure S2: Distribution of locally optimized parameters fit to individual clinical trials. A) Distribution of 50 parameter sets locally optimized to Motzer et al.[1] data. B) Distribution of 50 parameter sets locally optimized to Rakhit et al.[2] data. C) Distribution of 50 parameter sets locally optimized to Portielje et al.[3] data.

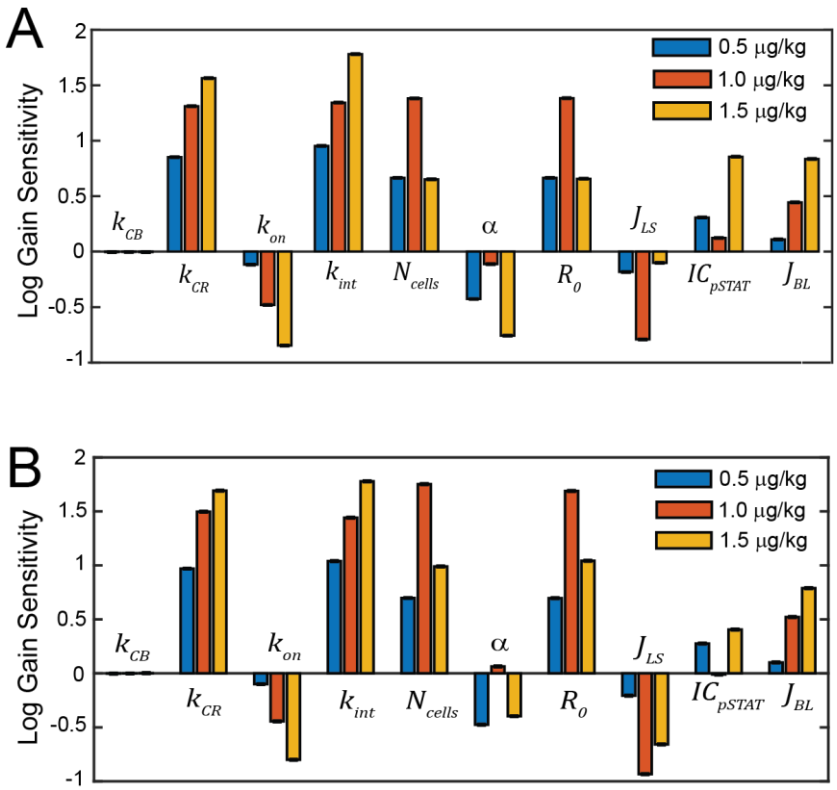

Supplemental Figure S3: Amount of desensitization predicted by reduced-bioavailability model sensitivities to relevant model parameters. A) Desensitization log gain sensitivities after two consecutive 1.0 μg/kg doses. B) Desensitization log gain sensitivities comparing desensitization after three consecutive 1.0 μg/kg doses. Sensitivities are calculated according to equation S33.

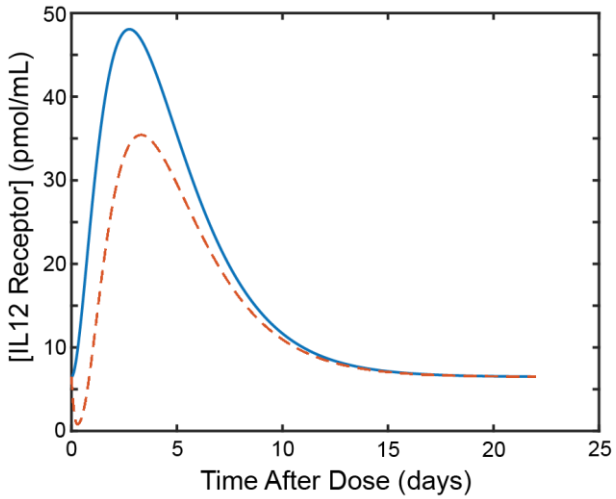

Supplemental Figure S4: Analytical approximation for receptor concentrations compared to numerical simulations for reduced-bioavailability model. Solid blue curve: analytical approximation. Dashed orange curve: numerical simulations.

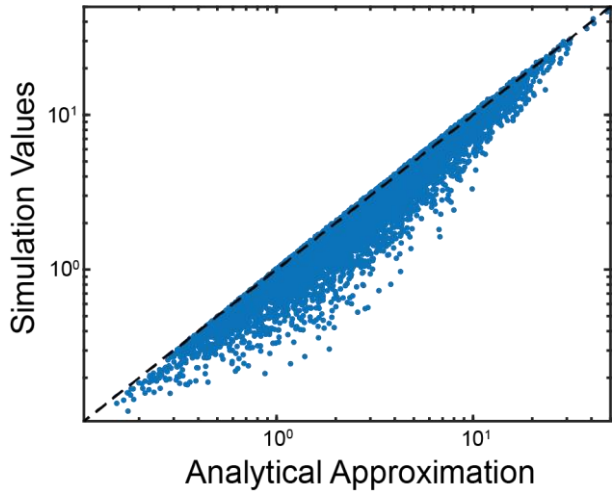

Supplemental Figure S5: Comparison of determined IL-12 binding flux ratio (equations 4.1 and 4.2) as calculated by numerical simulation and our analytical approximation for receptor dynamics.

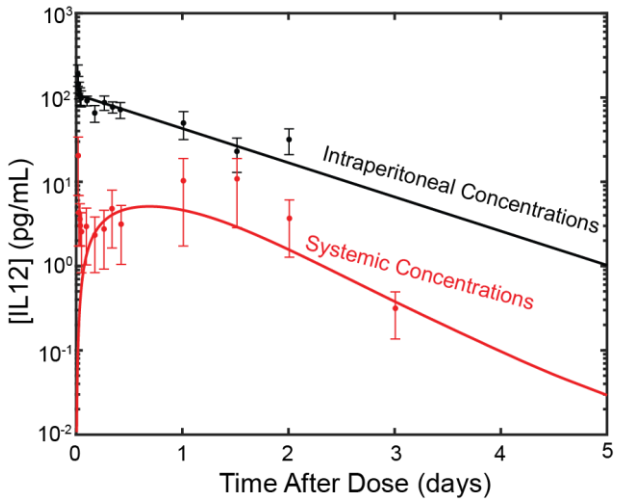

Supplemental Figure S6: Reduced-bioavailability model modified to represent IP injection of IL-12 fit to clinical trial data.

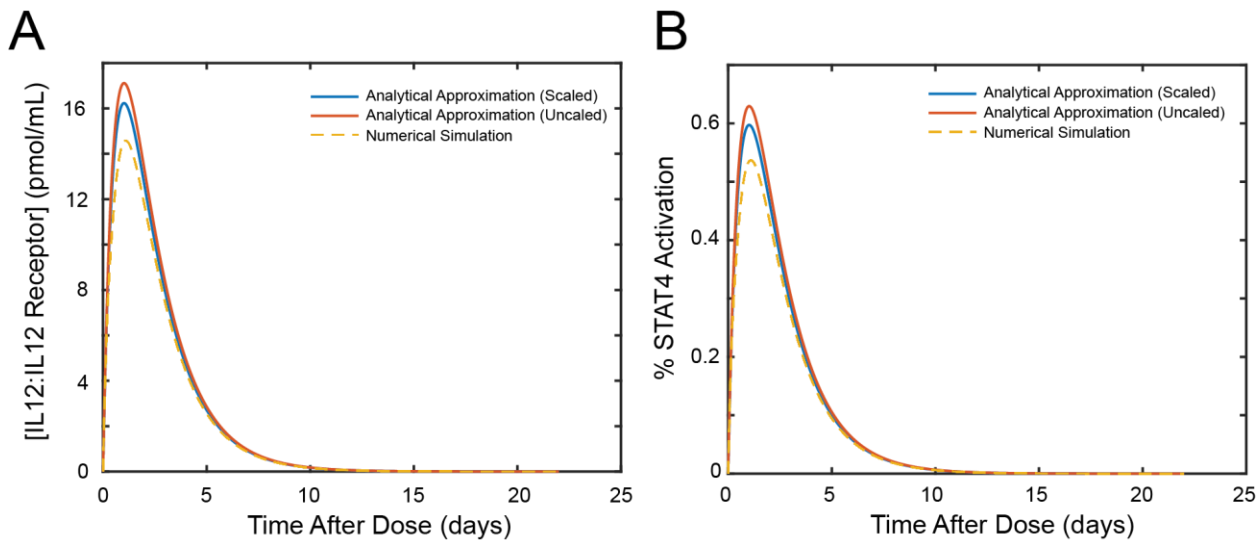

Supplemental Figure S7: Comparison of analytical approximation for the concentration of IL-12:IL-12 receptor and STAT4 activation in the reduced-bioavailability model. A) Predictions of complex concentrations. B) Predictions of STAT4 Activation. Blue curves: Scaled analytical approximations. Orange Curves: Unscaled analytical approximations. Dashed yellow curves: Numerically simulated values. See supplemental text for more information.

Supplementary Text

Contents

1. Derivation of Mathematical Models S14
   - 1.1 IL-12 Dosing S14
   - 1.2 IL-12 Transport Between Compartments S14
   - 1.3 IL-12 Receptor Binding and Complex Formation S16
   - 1.4 STAT4 Activation S16
   - 1.5 IL-12 Receptor Dynamics S17
   - 1.6 IL-12 Clearance S18
2. Model of Intraperitoneal IL-12 Injection S20
3. Model of Continuous, Local IL-12 Delivery S21
4. Local Model Sensitivity Analyses S21
5. Derivation of Analytical Approximation for Receptor Dynamics S22

Derivation of Mathematical Models

The two models used in this investigation are based on the same principles. The accelerated-clearance model consists of subcutaneous and serum compartments with receptor dynamics in the serum compartment. Similarly, the reduced-bioavailability model consists of the same two compartments with the addition of a lymphatic system compartment where IL-12 must travel before reaching the blood and receptor binding occurs. The equations governing IL-12 dosing, transport, clearance, binding, and signaling are equivalent for both models. In the following sections, we derive these terms. The descriptions and values for the parameters used in each model are located in supplementary tables S6 and S7.

IL-12 Dosing

In both models, IL-12 dosing occurs in the subcutaneous compartment. As the duration of injections is negligible compared to the simulation period, we model IL-12 dosing by setting the initial concentration of IL-12 in the subcutaneous space according to the following:

$$IL12_{S,0} = \frac{D}{V_S} \tag{S1}$$

Here, D is the dose amount administered in pmol and V_S is the volume of the subcutaneous space in mL.

IL-12 Transport Between Compartments

IL-12 transport between compartments is modeled based on a mass balance around each compartment and convective lymph fluid flow. As the molecular weight of IL-12 is greater than 16 kDa, transport to the blood from the subcutaneous space primarily occurs through lymph flow and, therefore, is unidirectional. Consider a simple two-compartment system where lymph flow

moves from compartment 1 to compartment 2 with volumetric flow rate j_{21} in mL days^{-1}. The mass balance around these two compartments are given by:

$$\frac{dV_1C_1}{dt} = -j_{21}C_1 \tag{S2}$$

$$\frac{dV_2C_2}{dt} = j_{21}C_1 \tag{S3}$$

where V_i is the volume of compartment i in mL and C_i is the concentration of IL-12 in compartment i in pmol mL^{-1}. We assume that the volume of each compartment remains constant, i.e., that fluid moving from each compartment is instantly replaced or removed. Accordingly, we can rearrange the two differential equations to become:

$$\frac{dC_1}{dt} = -\frac{j_{21}}{V_1}C_1 \tag{S4}$$

$$\frac{dC_2}{dt} = \frac{j_{21}}{V_2}C_2 \tag{S5}$$

Making the substitution $j_{21} = J_{21}V_1$, we further simplify to:

$$\frac{dC_1}{dt} = -J_{21}C_1 \tag{S6}$$

$$\frac{dC_2}{dt} = \frac{V_1}{V_2}J_{21}C_2 \tag{S7}$$

In these equations, J_{21} is the effective first order transport rate constant in days^{-1}. Conceptually, this parameter refers to the fluid flow leaving compartment 1 normalized by the volume of compartment 1. This framework is generalized to represent transport between all compartments in our model.

IL-12 Receptor Binding and Complex Formation

IL-12 binds its receptor either in the serum (accelerated-clearance model) or the lymphatic system (reduced-bioavailability model). For simplicity, we assume that binding is irreversible and occurs according to the rate law:

$$r_{binding} = k_{on}\ IL12_i\ R \tag{S8}$$

Here, k_{on} is the IL-12:IL-12 receptor association rate in mL pmol^{-1} days^{-1}, $IL12_i$ is the concentration of IL-12 in compartment i where receptor binding occurs, and R is the concentration of receptor both in pmol mL $^{-1}$. In our model both IL-12 and IL-12 receptor are consumed according to $r_{binding}$, and IL-12:IL-12 complex is generated at the same rate. Accordingly, the differential equation describing the concentration of IL-12:IL-12 receptor complex is given by:

$$\frac{dC}{dt} = k_{on}\ IL12_i\ R - k_{int}C \tag{S9}$$

Here, C is the concentration of IL-12:IL-12 receptor complex and k_{int} is the first order complex internalization rate constant in days^{-1}.

STAT4 Activation

In both models, the formation of IL-12:IL-12 receptor complex leads to activation of STAT4 based on the number of complexes per T-cell. Accordingly, we first calculate this quantity according to:

$$\tilde{C} = 6.023e11\frac{V_i C}{N_{cells}} \tag{S10}$$

where $\tilde{C}$ is the number of complexes per T-cell in # cells^{-1}, V_i is the volume of the compartment where binding occurs in mL, and N_{cells} is the number of T-cells in the compartment. The differential equation describing STAT4 activation is given by the following:

$$\frac{dpSTAT}{dt} = k_P\tilde{C}(1 - pSTAT) - k_{DP}\, pSTAT \tag{S11}$$

Here, pSTAT is the fraction of phosphorylated (activated) STAT4, k_p is the first order phosphorylation rate in cell #$^{-1}$ days^{-1}, and k_{DP} is the first-order dephosphorylation rate constant in days^{-1}. Furthermore, as intracellular processes are much faster than physiological processes such as transport and clearance, we assume that STAT4 activation is in quasi-steady state in our models. Thus, we can solve for pSTAT activation as the following:

$$pSTAT = \frac{k_P\tilde{C}}{k_P\tilde{C} + k_{DP}} = \frac{\tilde{C}}{\tilde{C} + \frac{k_{DP}}{k_P}} = \frac{\tilde{C}}{\tilde{C} + IC_{pSTAT}} \tag{S12}$$

where IC_{pSTAT} is the number of complexes per T-cell required for half-maximum STAT4 activation and is equivalent to $\frac{k_{DP}}{k_P}$.

IL-12 Receptor Dynamics

In the compartment where receptor binding occurs, we represent the concentration of receptor based on a basal production rate, an upregulated production rate based on STAT4 activation, consumption via binding, and unbound internalization/clearance. Accordingly, the differential equation describing the concentration of receptor is given by:

$$\frac{dR}{dt} = \frac{N_{cells}}{V_i}k_R + \frac{N_{cells}}{V_i}\,\alpha\, pSTAT - k_{on}\, IL12_I\, R - k_{CR}R \tag{S13}$$

where k_R is the basal production rate per T-cell in pmol cells^{-1} days^{-1}, k_{CR} is the unbound receptor internalization rate in days $^{-1}$, and α is the feedback parameter representing upregulated

receptor production by STAT4 activation in pmol cells^{-1} days^{-1}. Furthermore, we set the steady state concentration of receptor according to the following relationship:

$$R_{SS} = \frac{R_0 N_{cells}}{V_i} \tag{S14}$$

Here, R_{ss} is the steady state/initial concentration of receptor in the absence of any IL-12 and R_0 is the basal number of IL-12 receptors per T-cell in the absence of IL-12 and STAT4 activation. To ensure that the concentration of receptor remains at this level at steady state, we constrain the basal production rate k_R according to:

$$k_R = R_0 k_{CR} \tag{S15}$$

IL-12 Clearance

In addition to receptor mediated clearance, IL-12 can exit the body in our model via degradation in the subcutaneous space or traditional serum clearance. Clearance from the serum is determined by the first order clearance rate constant k_{CB} in days^{-1}. Instead of directly specifying the degradation rate of IL-12 in the subcutaneous space, we specify the absolute bioavailability (fraction of IL-12 in the subcutaneous space that does not get degraded) and determine the corresponding degradation rate. Accordingly, degradation of IL-12 in the subcutaneous space is determined by:

$$k_{DG} = \frac{1 - F}{F} J_{iS} \tag{S16}$$

where k_{DG} is the first order subcutaneous degradation rate constant and J_{iS} is the first order transport rate constant from the subcutaneous space to compartment *i,* both in days^{-1}. In the

accelerated-clearance model, this transport rate is that of IL-12 to the blood and in the reduced bioavailability model it is that of IL-12 to the lymphatic system.

Model of Intraperitoneal IL-12 Injection

We developed the reduced-bioavailability model to simulate subcutaneous dosing of IL-12; thus, we modified our model slightly to fit intraperitoneal injection data presented by Lenzi et al.[8]. All model equations here are identical to the original model equations (other than slight notation changes) except the equation determining the initial concentration of IL-12 in the intraperitoneal cavity. In the clinical trial data presented by Lenzi and colleagues, the initial concentration of IL-12 in the intraperitoneal cavity is two orders of magnitude lower than what is expected given the reported dose amount. To account for this, we add the scaling factor β to our expression for the initial concentration of IL-12 in the intraperitoneal cavity to obtain equation S17.

$$IL12_{P,0} = \beta \frac{D}{V_P} \tag{S17}$$

Here, β is a factor between zero and one that accounts for the discrepancy between the reported dose and initial concentrations of IL-12. Adding in this change and changes in notation to reflect IL-12 administration to the peritoneal cavity, we obtain equations S18-27

$$\frac{dIL12_P}{dt} = -J_{LP}\, IL12_P - k_{DG}\, IL12_P \tag{S18}$$

$$\frac{dIL12_L}{dt} = \frac{J_{LP}V_P}{V_L}\, IL12_P - k_{on}\, IL12_L\, R - J_{BL}\, IL12_L \tag{S19}$$

$$\frac{dR}{dt} = \frac{N_{cells}}{V_L} k_R + \frac{N_{cells}}{V_L}\, \alpha\, pSTAT - k_{on} IL12_L R - k_{CR} R \tag{S20}$$

$$\frac{dC}{dt} = k_{on}\, IL12_L\, R - k_{int} C \tag{S21}$$

$$\frac{dIL12_B}{dt} = \frac{J_{BL}V_L}{V_B}\, IL12_L - k_{CB}\, IL12_B \tag{S22}$$

$$\tilde{C} = \frac{6.023e11V_L}{N_{cells}} C \tag{S23}$$

$$pSTAT = \frac{\tilde{C}}{\tilde{C} + IC_{pSTAT}} \tag{S24}$$

$$k_R = k_{CR}R_0 \tag{S25}$$

$$k_{DG} = \frac{(1-F)}{F} J_{LS} \tag{S26}$$

$$IL12_{P,0} = \beta \frac{D}{V_P} \tag{S27}$$

Model of Continuous, Local IL-12 Delivery

We further modified our model to represent continuous, local delivery of IL-12 within the intraperitoneal cavity. All equations in this model are identical to that of intraperitoneal injection of IL-12 except for the equations governing IL-12 in the intraperitoneal space. Here, the ordinary differential equation describing the concentration of IL-12 in the intraperitoneal space is now given by equation S28.

$$\frac{dIL12_P}{dt}\, k_{pr}(t) - J_{LP}\, IL12_P - \, k_{DG}\, IL12_P \tag{S28}$$

Here, $k_{pr}(t)$ is the 0th order production rate of IL-12 that varies with time according to the dosing strategy being simulated in pmol days^{-1}. We test three different dosing strategies designed to reach equivalent i.p. concentrations at long times: 1) constant production, 2) stepwise production, and 3) linearly increasing production. These production profiles are given by equations S29, S30, and S31, respectively.

$$k_{prod}(t) = \begin{cases} 0, & t < t_1 \\ k_{pr}^{f}, & t \geq t_1 \end{cases} \tag{S29}$$

$$k_{prod}(t) = \begin{cases} \frac{1}{3}k_{pr}^{f}, & t_1 \leq t \leq t_2 \\ \frac{1}{2}k_{pr}^{f}, & t_2 < t \leq t_3 \\ k_{pr}^{f}, & t > t_3 \end{cases} \tag{S30}$$

$$k_{prod}(t) = \begin{cases} 0, & t < t_1 \\ \frac{k_{pr}^{f} - k_{pr}^{0}}{t_2 - t_1}(t - t_1), & t_1 \leq t \leq t_2 \\ k_{prod}^{f}, & t > t_2 \end{cases} \tag{S31}$$

In the equations above k_{pr}^{f} is the final production rate reached by each production profile, and t_1 is the time at which dosing begins. The stepwise production profile is further characterized by t_2 and t_3, which are the times where IL-12 production is increased. Similarly, the linearly increasing production profile is characterized by t_1 and t_2, the time in which the increase in production rate begins and ends, respectively. All characteristic times of dosing profiles are given in days. Additionally, the initial production rate here is defined by k_{pr}^{0}.

<u>Local Model Sensitivity Analyses</u>

Local sensitivity analyses were implemented to determine the impact of model parameters on the extent of IL-12 PK desensitization. For the simulation of multiple repeated doses of the same amount, we quantify the amount of desensitization predicted as the ratio of IL-12 serum AUC after the last and first dose according to equation S32.

$$\chi = \frac{AUC_{last}}{AUC_{first}} \tag{S32}$$

To determine the sensitivity of the quantity χ to a given parameter p, we calculated the log gain sensitivity according to equation S33.

$$S = \frac{\partial \ln(\chi)}{\partial \ln(p)} = \frac{\Delta \ln(\chi)}{\Delta \ln(p)} \tag{S33}$$

Derivation of Analytical Approximation for Receptor Dynamics

To approximate the concentration of IL-12 receptor in the reduced-bioavailability model over time with an analytical expression, we aimed to approximate species in the model with exponential expressions. As the upregulation of receptor is regulated by the amount of STAT4 activation in T-cells, which is in turn regulated by the amount of IL-12:IL-12 receptor, we start by approximating the amount of complex formation that occurs in the lymphatic system. The ordinary differential equation describing the concentration of complex formed is given in equation S2.5. Importantly, this differential equation is nonlinear due to the $k_{on} IL12_L R$ term. As a linear approximation, we assume that the binding flux is equal to the flux into the lymphatic system such that $k_{on}\, IL12_L\, R = \frac{J_{LS} V_S}{V_L}\, IL12_S$, giving us equation S34.

$$\frac{dC}{dt} = \frac{J_{LS} V_S}{V_L}\, IL12_S - k_{int} C \tag{S34}$$

The concentration of IL-12 in the subcutaneous space, $IL12_S$, is described by a single exponential decay since for this model we fix $F = 1$. Equation S35 contains the exponential decay describing the concentration of IL-12 in the subcutaneous space.

$$IL12_S(t) = \frac{D}{V_S} \exp\{-J_{LS} t\} \tag{S35}$$

Making this substitution allows us to solve equation S32 analytically, giving the dual exponential decay found in equation S36.

$$C(t) = \frac{J_{LS} D}{(k_{int} - J_{LS}) V_L} [\exp\{-J_{LS} t\} - \exp\{-k_{int} t\}] \tag{S36}$$

Based on equations 15 and 16 in the main text, we can now approximate the level of STAT4 activation according to equation S37.

$$pSTAT(t) = \frac{\frac{6.023e11V_L}{N_{cells}}C(t)}{\frac{6.023e11V_L}{N_{cells}}C(t) + IC_{pSTAT}} \tag{S37}$$

These approximations for the concentration of complex and STAT4 activation are in reasonable agreement with numerical simulations as seen in supplemental figure S7 (orange curves). However, there is a slight overprediction of both species likely due to our assumption that binding flux is equal to the total flux of IL-12 into the lymphatic system. To account for this difference, we rescale our approximation for the amount of complex formed by the initial ratio of binding flux to total flux, such that $C(t)$ is now given by equation S38.

$$C(t) = \frac{\frac{k_{on}R_0N_{cells}}{V_L}}{\frac{k_{on}R_0N_{cells}}{V_L} + J_{BL}} \frac{J_{LS}D}{(k_{int} - J_{LS})V_L}[\exp\{-J_{LS}t\} - \exp\{-k_{int}t\}] \tag{S38}$$

As seen in supplemental figure S7 (blue curves), this slightly increases the accuracy of our analytical approximations compared to numerical simulations. Using equation S37 and S38, we can now solve for an analytical approximation for the concentration of receptor in the lymphatic system. This ordinary differential equation is listed in equation 12 in the main text, but we must make two modifications to linearize this equation. Here, we make an important assumption that at long times (around the time of the next dose, which is our time span of interest), the amount of IL-12 in the lymphatic system is negligible such that $k_{on}IL12_LR \approx 0$. Additionally, our expression for $pSTAT(t)$ is non-linear; however, in the parameter regime we are operating $IC_{pSTAT} \gg \frac{6.023e11V_L}{N_{cells}}C(t)$, thus we can assume this function is approximately linear as given by equation S37.

$$pSTAT(t) = \frac{6.023e11V_L}{N_{cells}\, IC_{pSTAT}} C(t) \tag{S39}$$

Thus, our ordinary differential equation for receptor concentrations in the lymphatic system becomes linear, given by equation S38.

$$\frac{dR}{dt} = \frac{N_{cells}k_R}{V_L} + \frac{N_{cells}\alpha}{V_L}\frac{6.023e11V_L}{N_{cells}\, IC_{pSTAT}} C(t) - k_{CR}R \tag{S40}$$

This ordinary differential equation can be solved analytically and making the important substitution $k_R = k_{CR}R_0$ given by equation 17 in the main text, we obtain equation S41-S45.

$$R(t) = \frac{R_0 N_{cells}}{V_L} + e_1(t) + e_2(t) + e_3(t) \tag{S41}$$

$$e_1(t) = \frac{\Phi exp\,(-J_{LS}t)}{(J_{LS} - k_{int})(J_{LS} - k_{CR})} \tag{S42}$$

$$e_2(t) = \frac{\Phi \exp(-k_{int}t)}{(k_{int} - J_{LS})(k_{int} - k_{CR})} \tag{S43}$$

$$e_3(t) = \frac{\Phi \exp\,(-k_{CR}t)}{(k_{CR} - k_{int})(k_{CR} - J_{LS})} \tag{S44}$$

$$\Phi = \frac{6.023e11k_pJ_{LS}\alpha D}{V_L k_{DP}} \frac{\frac{k_{on}R_0N_{cells}}{V_L}}{\frac{k_{on}R_0N_{cells}}{V_L} + J_{BL}} \tag{S45}$$

References

1. Motzer RJ, Rakhit A, Schwartz LH, et al. Phase I trial of subcutaneous recombinant human interleukin-12 in patients with advanced renal cell carcinoma. *Clinical Cancer Research*. 1998;4(5):1183-1191.

2. Rakhit A, Yeon MM, Ferrante J, et al. Down-regulation of the pharmacokinetic-pharmacodynamic response to interleukin-12 during long-term administration to patients with renal cell carcinoma and evaluation of the mechanism of this "adaptive response" in mice. *Clinical Pharmacology & Therapeutics*. 1999;65(6):615-629. doi:10.1016/S0009-9236(99)90083-8

3. Portielje JEA, Kruit WHJ, Schuler M, et al. Phase I Study of Subcutaneously Administered Recombinant Human Interleukin 12 in Patients with Advanced Renal Cell Cancer. *Clinical Cancer Research*. 1999;5(12):3983-3989.

4. Chizzonite R, Truitt T, Desai BB, et al. IL-12 receptor. I. Characterization of the receptor on phytohemagglutinin-activated human lymphoblasts. *The Journal of Immunology*. 1992;148(10):3117-3124. doi:10.4049/jimmunol.148.10.3117

5. Sender R, Weiss Y, Navon Y, et al. The total mass, number, and distribution of immune cells in the human body. *Proceedings of the National Academy of Sciences*. 2023;120(44):e2308511120. doi:10.1073/pnas.2308511120

6. Milewski M, Manser K, Nissley BP, Mitra A. Analysis of the absorption kinetics of macromolecules following intradermal and subcutaneous administration. *European Journal of Pharmaceutics and Biopharmaceutics*. 2015;89:134-144. doi:10.1016/j.ejpb.2014.11.013

7. Varkhede N, Forrest ML. Understanding the Monoclonal Antibody Disposition after Subcutaneous Administration using a Minimal Physiologically based Pharmacokinetic Model. *J Pharm Pharm Sci*. 2018;21(1 Suppl):130s-148s. doi:10.18433/jpps30028

8. Lenzi R, Rosenblum M, Verschraegen C, et al. Phase I Study of Intraperitoneal Recombinant Human Interleukin 12 in Patients with Müllerian Carcinoma, Gastrointestinal Primary Malignancies, and Mesothelioma1. *Clinical Cancer Research*. 2002;8(12):3686-3695.